

# Effects of the Reynolds Number and Prandtl Number on Flow and Temperature Field inside a Square Vented Enclosure having Heat Conducting Block

M. U. Ahammad<sup>1</sup>, M. M. K. Chowdhury<sup>2</sup>, M. M. Rahman<sup>3</sup>

<sup>1</sup>Department of Mathematics, Dhaka University of Engineering and Technology (DUET), Gazipur-1700, Bangladesh

<sup>2,3</sup>Department of Mathematics, Bangladesh University of Engineering and Technology (BUET), Dhaka-1000, Bangladesh

## ABSTRACT

An approach is performed following finite element technique for MHD flow of viscous incompressible and electrically conducting fluid around a heat conducting solid block placed in a ventilated enclosure. A uniform transverse magnetic field is imposed in the opposite direction of flow perpendicular to the right vertical wall. Reynolds number and Prandtl number effects are investigated on flow and thermal field at a wide range of Reynolds ( $50 \leq Re \leq 500$ ) and Prandtl ( $0.071 \leq Pr \leq 7.1$ ) numbers. The expressions for the flow visualizations and temperature distributions inside the studied domain are presented by streamlines and isotherms. Moreover average Nusselt number at the hot wall and average bulk fluid temperature in the cavity are obtained. It is observed that the results focused in this paper are consistent with the physical reality of the flow problem.

**Keywords:** Reynolds Number, Prandtl Number, Square Enclosure, Mixed Convection, Heat Conduction.

## I. INTRODUCTION

Simultaneous free and forced convection in different geometries has many engineering and industrial applications such as cooling of electronic equipments, thermal insulation, air conditioning, heat exchangers, drying or geophysics studies. In modern days, the probable utilization of magnetohydrodynamic (MHD) is to affect a flow stream of an electrically conducting fluid for the purpose of thermal protection, propulsion and control. To realize the MHD convective heat transfer of electrically conducting fluids in cavities has been found an increasing interest in many literatures.

Natural convection in a rectangular cavity of electrically conducting fluid with energy sources and sinusoidal temperature at the bottom wall was presented by Obayedullah et al. [9]. Rahman et al. [12] performed an analysis of MHD mixed convection in a horizontal channel with an open cavity. Ahammad et al. [2] investigated the effect of inlet and outlet

openings in a vented cavity having a heat generating square block. Later on a study on combined free and forced convection flow and heat transfer manners in a ventilated enclosure in the presence of heat generating obstacle has been carried out by Ahammad et al [3]. Rahman et al. [11] studied the problem of mixed convection flow inside a rectangular cavity vented with a centered heat conducting square cylinder. The fluid flow characteristic of combined convection in a lid-driven cavity with a circular body where the left wall of the cavity was heated has been analyzed by Oztop et al. [6]. Saeidi and Khodadadi [15], presented a steady laminar forced convection flow problem in a square cavity with inlet and exit ports. Very recently, Prakash and Ravikumar [1] investigated the thermal comfort in a room with windows at adjacent walls along with additional vents.

The opposing mixed convection in a rectangular cavity heated from the side with a constant heat flux using the finite difference method for the assisting forced flow patterns was performed by Raji and Hasnaoui

[13]. The combined forced and free convection in a square vented cavity containing a heat conducting horizontal solid circular cylinder was studied by Rahman et al. [10]. For a lid-driven blocked enclosure; Billah et al. [4] performed a simulation of MHD mixed convection heat transfer enhancement. Natural convective flow in a rectangular enclosure having electrically conducting fluid with a magnetic field was reported by Mehmet and Elif [8] to find the inclination effect of the enclosure. Gau et al. [5] studied an experimental work on mixed convection in a horizontal rectangular channel heated from a side. Kumar and Dalal [7] analyzed natural convection around a heated square cylinder placed in an enclosure for the Reynolds number in the range  $10^3 \leq Re \leq 10^6$ . They focused the fact that the uniform wall temperature heating is quantitatively dissimilar from the uniform wall heat flux heating.

The objective of the present work is to characterize the flow and thermal characteristic of fluid (air) placed in the enclosure at different Reynolds numbers and Prandtl numbers together with a heat conducting solid block located at the center of the cavity.

## II. METHODS AND MATERIAL

### 2. Details of Studied Area

The physical model of the studied problem shown in Figure 1 that consists of a square cavity of length  $L$  with a heat conducting solid block located at the center. Except the bottom surface which is kept at a constant temperature  $T_h$  all sides of the cavity were taken as thermally isolated. The inlet port is placed on the bottom of the left wall, exit port is situated at the top of the right wall and the magnitude of each port is  $w = 0.1L$ . For all solid boundaries rigid no-slip walls assumed that is velocity components  $u$  and  $v$  are set to be zero. The flow of a uniform velocity,  $u_i$  and the ambient temperature,  $T_i$  enters into the cavity and the outgoing flow is considered to have zero diffusion flux for all dependent variables.

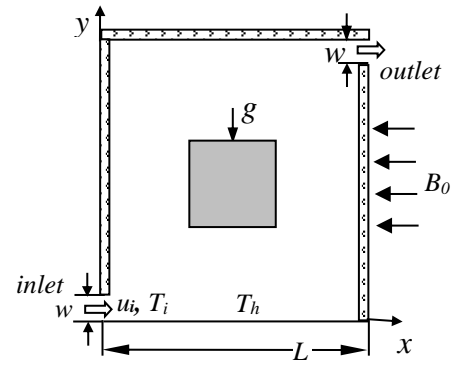


**Figure 1.** The physical domain used for numerical simulation

For a steady state, two-dimensional, laminar, incompressible flow of a Newtonian and electrically conducting fluid with constant thermophysical properties, the governing differential equations designed for the present problem in the dimensionless form consisting of the conservation of mass, momentum, and energy can be expressed as

$$\frac{\partial U}{\partial X} + \frac{\partial V}{\partial Y} = 0 \quad (1)$$

$$U \frac{\partial U}{\partial X} + V \frac{\partial U}{\partial Y} = -\frac{\partial P}{\partial X} + \frac{1}{Re} \left( \frac{\partial^2 U}{\partial X^2} + \frac{\partial^2 U}{\partial Y^2} \right) \quad (2)$$

$$U \frac{\partial V}{\partial X} + V \frac{\partial V}{\partial Y} = -\frac{\partial P}{\partial Y} + \frac{1}{Re} \left( \frac{\partial^2 V}{\partial X^2} + \frac{\partial^2 V}{\partial Y^2} \right) + Ri \theta - \frac{Ha^2}{Re} V \quad (3)$$

$$U \frac{\partial \theta}{\partial X} + V \frac{\partial \theta}{\partial Y} = \frac{1}{Re Pr} \left( \frac{\partial^2 \theta}{\partial X^2} + \frac{\partial^2 \theta}{\partial Y^2} \right) \quad (4)$$

For heat conducting solid block

$$\left( \frac{\partial^2 \theta_s}{\partial X^2} + \frac{\partial^2 \theta_s}{\partial Y^2} \right) = 0 \quad (5)$$

where  $Re = \frac{u_i L}{\nu}$  is the Reynolds number,  $Pr = \frac{\nu}{\alpha}$  is the

Prandtl number,  $Ha = B_0 L \sqrt{\frac{\sigma}{\mu}}$  is the Hartmann

number,  $Ri = \frac{Gr}{Re^2}$  is the Richardson number,  $K = \frac{k_s}{k}$

is the solid fluid thermal conductivity ratio,

$\Delta T = T_h - T_i$  is the temperature difference  $\alpha = \frac{k}{\rho C_p}$  is

the thermal diffusivity of the fluid.

**Boundary Conditions:** The non-dimensional boundary conditions which are used in the current work can be set as follows:-

$U = 1, V = 0, \theta = 0$  at the inlet

$P = 0$  at the outlet: convective boundary condition (CBC)

$\theta = 1$  at the bottom heated surface

$U = 0, V = 0, \frac{\partial \theta}{\partial N} = 0$  at the left, right and top walls

$$\left(\frac{\partial \theta}{\partial N}\right)_{fluid} = K \left(\frac{\partial \theta_s}{\partial N}\right)_{solid} \text{ at the solid-fluid interfaces}$$

The average Nusselt number  $Nu$  at the hot wall is given by

$$Nu_{av} = - \int_0^1 \left(\frac{\partial \theta}{\partial Y}\right) dX$$

and the bulk average fluid temperature in the enclosure is defined as

$$\theta_{av} = \int \theta \frac{d\bar{V}}{V}, \text{ where } \bar{V} \text{ is the cavity volume.}$$

The computational procedure is similar to the works performed by Ahammad et al. [2, 3]. The governing nonlinear mass, momentum and energy equations are solved numerically by finite element method with Galerkin weighted residual scheme.

### 3. Model Validation Data

Different grid sizes of 2312, 3976, 5158, 6278 and 7724 elements are taken for the present simulation to test the independency of the results with the grid variations. Average Nusselt number at the heated surface and average fluid temperature in the cavity are examined for these selected elements. From Table 1 it is seen that the variations among the results are very minor for different numbers of elements. Here the grid consisting of 5158 elements are chosen considering both the accuracy of the numerical values and the computational time throughout the simulation.

Table 1. Grid refinement test at  $Ri = 1.0, Ha = 10.0, Re = 100$  and  $Pr = 0.71$

Elements	2312	3976	5158	6278	7724
$Nu$	5.895421	5.992341	6.025271	6.050949	6.061874
$\theta$	0.688475	0.689856	0.691123	0.691209	0.691713

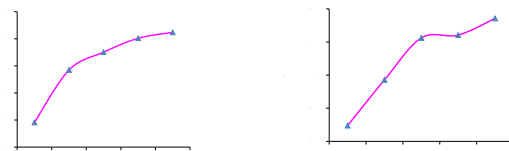


Figure 2. Grid test shows average Nusselt number and average fluid temperature

For the numerical code validation of the current study, a computation is carried out to compare with the numerical study of mixed convection problem in a lid-driven enclosure having a circular body by Oztop et al. [6]. Figure 3 shows the relationships between the works of Oztop et al. [6] and present with good agreement in streamlines and isotherms.

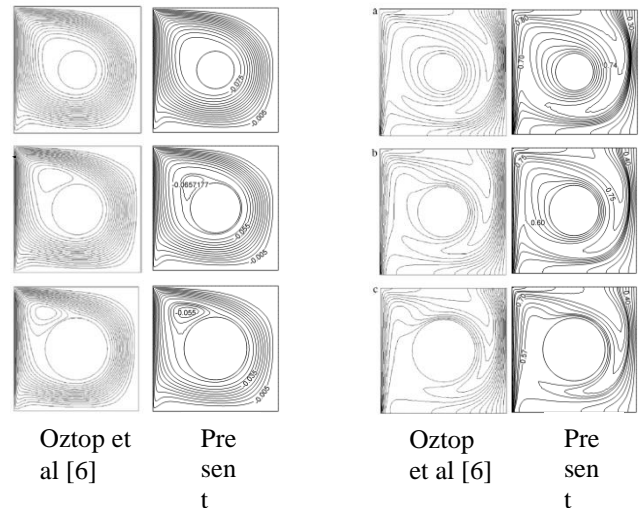


Figure 3. Comparison of streamlines and isotherms for (a)  $D = 0.3L$ , (b)  $D = 0.4L$  and (c)  $D = 0.5L$  while  $Gr = 10^5, Pr = 0.71, C = 0.5$  and  $Re = 1000$

### III. RESULTS AND DISCUSSION

In order to investigate the flow behaviors, thermal fields and heat transfer performance affected by the Reynolds number and Prandtl number, a mixed convection problem in a vented enclosure with heat conductive block has been performed numerically.

The influence of Reynolds number on the overall flow pattern and heat lines arrangements are depicted in Figures 4 and 5. Here the value of  $Pr$  is chosen as 0.71 which corresponds to air. These figures show the

streamlines and isotherm contours for various Reynolds number varied from 50 to 500. From Figure 4 it is observed that at low Reynolds number  $Re=50$ , the mainstream occupies the whole domain for  $Ri=(0.1, 1)$  whereas a very large counter clockwise vortex is developed confining the centered block for  $Ri=10$ . When  $Re=200$ , a unicellular vortex is found above the inlet opening and it expands very sharply for the higher values of  $Ri$ . In the dominant forced convection region a very big sized anticlockwise rotating cell is created and another small clockwise vortex is seen at the right bottom corner for  $Re=350$ . Large vortex swells up and small one disappears as  $Ri$  increases. At  $Re=500$  a minor change is followed in flow patterns with the comparison of  $Re=350$ .

The corresponding isotherms for different Reynolds numbers are displayed in Figure 5. For the lower value of  $Re=50$  the heat lines are nonlinear that stretched the whole cavity and a small variation is noticed for different values of Richardson numbers. The isotherms are packed at the inlet and form a boundary layer in the vicinity of bottom hot wall of the cavity at  $Re=200$ . As the Reynolds number increases ( $Re=350, 500$ ) the isothermal lines move away to the right wall and high isotherms are crowded at the heated surface of the cavity. In the case of two upper values of  $Ri$  (1, 10), a tendency is observable for the low temperature heatlines is coming back towards the left wall of the enclosure.

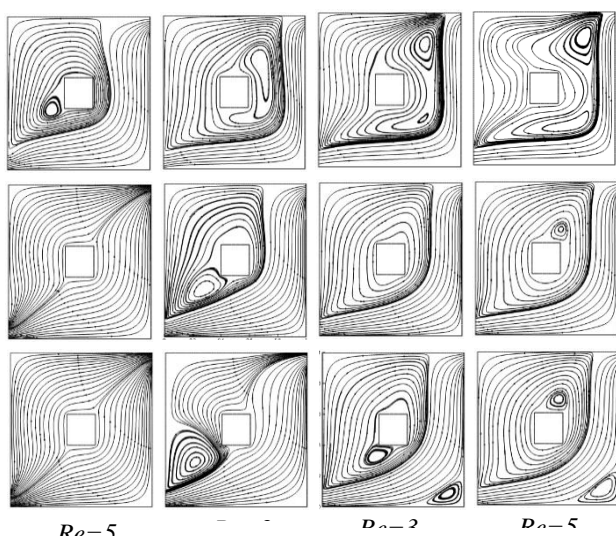


**Figure 4.** Streamlines for different values of  $Re$  and  $Ri$ , with  $Ha=10$  and  $Pr=0.71$

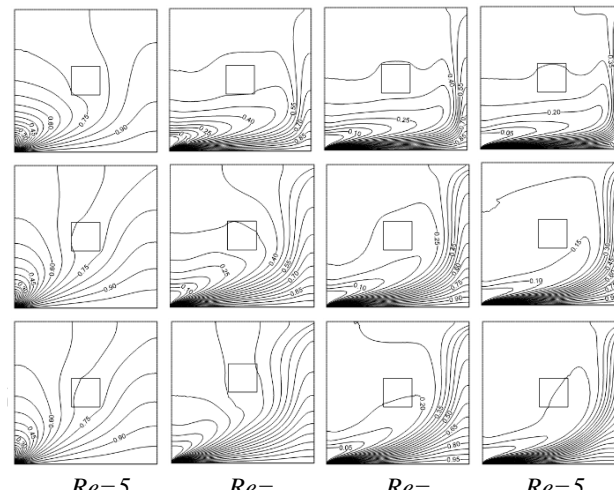


**Figure 5.** Isotherms for different values of  $Re$  and  $Ri$ , with  $Ha=10$  and  $Pr=0.71$ .

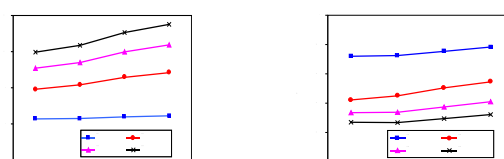


**Figure 6.** Average Nusselt number and average fluid temperature versus Richardson number for different values of Reynolds number

Figure 6 illustrates average Nusselt number at the heated wall and bulk average fluid temperature in the cavity for different values of  $Re$ . It is seen that for low Reynolds number heat transfer rate at the bottom wall is about stationary with respect to  $Ri$  and maximum heat transfer is found for the largest value of  $Re$  which is reasonable. A reverse effect is followed for the case of average temperature of the fluid inside the cavity.

To consider the effects of Prandtl number in the range 0.071-7.1 on flow and thermal fields inside a vented enclosure with heat conductive block placed at the center, the other parameters are kept fixed at  $Re = 100$  and  $Ha = 10$ . The flow characteristics that are represented by streamlines for four different values of Prandtl number are shown in Figure 7. At  $Ri=0.1$  and for all selected values of  $Pr$  it is seen that a recirculation cell is formed just above the inflow opening and open lines are identical. There is no significant change except extended vortex size is observed for the different Prandtl numbers in the case of pure mixed convection  $Ri=1$ . But when  $Ri=10$  a dramatically variation in flow patterns is noticed for the studied Prandtl numbers. Major streams minimize

towards the right-bottom walls and consequently size of the various shaped vortices expand very swiftly and surrounded the inner block.

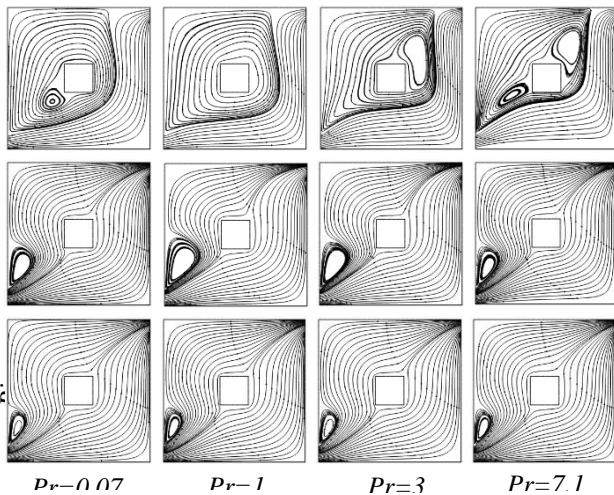


**Figure 7.** Streamlines for different values of  $Pr$  and  $Ri$ , with  $Ha=10$  and  $Re=100$ .

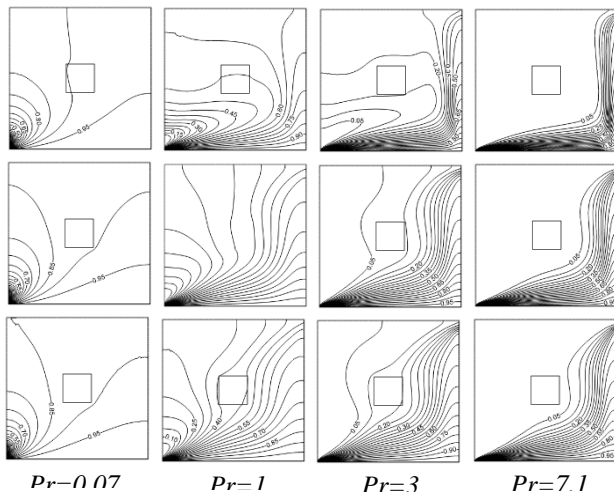


**Figure 8.** Isotherms for different values of  $Pr$  and  $Ri$ , with  $Ha=10$  and  $Re=100$ .

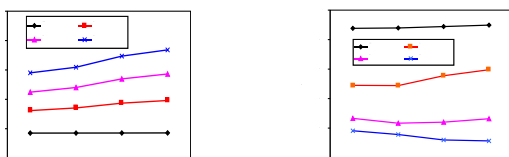


**Figure 9.** Average Nusselt number and average fluid temperature versus Richardson number for different values of Prandtl number

In order to examine the mode of temperature distribution heatline contours are plotted in Figure 8. At  $Pr = 0.071$  a small number of high isotherms only are observed for all the considered values of  $Ri$ . On the other hand, for  $Ri = 0.1, 1, \text{ and } 10$  temperature distributions are followed almost the whole domain

with thermal boundary layer at the bottom wall when  $Pr = 1$ . As Prandtl number increases a noteworthy change occurs in the isotherms pattern. For larger values of  $Pr (=3, 7.1)$  hot wall is jammed by heatlines and gradually these became isolate from the heat conducting solid in the case of all chosen Richardson numbers.

Lastly average heat transfer rate is presented in Figure 9 along the heated wall at different Prandtl numbers. Heat transfer rate is highest and it slowly rises up with increasing of Richardson number when  $Pr=7.1$ . Also it follows that smallest value of  $Pr$  gives minimum heat transfer which is independent of  $Ri$ . On the other hand, average temperature of fluid inside the enclosure decreases as Prandtl number increases.

#### IV. CONCLUSION

In this study, combined free and forced convective flows with thermal fields affected by the Reynolds and Prandtl numbers have been investigated.

- The results show that there is a considerable enhancement in heat transfer from the heated wall due to higher values of Reynolds number.
- Prandtl number effects in flow behaviors are more significant in free convection dominated region than other two regimes. Heat transfer at the bottom heated surface increases with increasing of Prandtl number.

#### V. REFERENCES

- [1] Prakash, D. and Ravikumar, P., (2013). Study of thermal comfort in a room with windows at adjacent walls along with additional vents, Indian Journal of Science and Technology, 6(6), 4659-4669.
- [2] Ahammad, M. U., Rahman, M. M., Rahman, M. L., (2012). Effect of inlet and outlet position in a ventilated cavity with a heat generating square block, Engineering e-Transaction, 7(2), 107-115.
- [3] Ahammad, M. U., Rahman, M. M., Rahman, M. L., (2013). Mixed Convection Flow and Heat Transfer Behavior inside a Vented Enclosure in the Presence of Heat Generating Obstacle, International Journal of Innovation and Applied Studies, 3(4), 967-978.

- [4] Billah, M.M., Rahman, M.M., Saidur, R., Hasanuzzaman, M., (2011). Simulation of MHD mixed convection heat transfer enhancement in a double lid-driven obstructed enclosure, *International Journal of Mechanical and Materials Engineering*, 6(1), 18-30.
- [5] Gau, C., Jeng, Y.C., Liu, C.G., (2000). An experimental study on mixed convection in a horizontal rectangular channel heated from a side, *ASME J. Heat Transfer*, 122, 701-707.
- [6] Oztop, H.F., Zhao, Z., Yu, B., (2009). Fluid flow due to combined convection in lid-driven enclosure having a circular body, *Int. J. Heat and Fluid Flow*, 30, 886-901.
- [7] Kumar, De, A., Dalal, A. (2006). A numerical study of natural convection around a square horizontal heated cylinder placed in an enclosure, *International journal Heat Mass Transfer*, 49, 4608-4623.
- [8] Mehmet, C.E. and Elif, B., (2006). Natural convection flow under a magnetic field in an inclined rectangular enclosure heated and cooled on adjacent walls, *Fluid Dynamics Research*, 38, 564-590.
- [9] Obayedullah, M., Chowdhury, M.M.K. and Rahman, M.M., (2013). Natural convection in a rectangular cavity having internal energy sources and electrically conducting fluid with sinusoidal temperature at the bottom wall, *International Journal of Mechanical and Materials Engineering*, 8(1), 73-78.
- [10] Rahman, M.M., Alim, M.A., Saha, S., Chowdhury, M.K., (2008). Mixed convection in a vented square cavity with a heat conducting horizontal solid circular cylinder, *Journal of Naval Architecture and Marine Engineering*, 5(2), 37-46.
- [11] Rahman, M.M., Elias, M., Alim, M.A., (2009). Mixed convection flow in a rectangular ventilated cavity with a heat conducting square cylinder at the center, *J. of Engineering and Applied Sciences*, 4(5), 20-29.
- [12] Rahman, M. M., Parvin, S. Saidur, R., Rahim, N. A., (2011). Magnetohydrodynamic mixed convection in a horizontal channel with an open cavity, *International Communication Heat Mass Transfer*, 38, 184-193.
- [13] Raji, A., Hasnaoui, M., (1998). Mixed convection heat transfer in a rectangular cavity ventilated and heated from the side, *Numer Heat Transfer, Part A*, 33, 533-548.
- [14] Reddy, J.N., (1993). *An Introduction to Finite Element Analysis*, McGraw-Hill, New-York.
- [15] Saeidi, S.M., Khodadadi, J.M., (2006). Forced convection in a square cavity with inlet and outlet ports, *Int. J. of Heat and Mass Transfer*, 49, 1896-1906.

### Nomenclature

- $B_0$  magnetic induction ( $Wb/m^2$ )
- $g$  gravitational acceleration ( $ms^{-2}$ )
- $Gr$  Grashof number
- $h$  convective heat transfer coefficient ( $Wm^{-2}K^{-1}$ )
- $Ha$  Hartmann number
- $k$  thermal conductivity of fluid ( $Wm^{-1}K^{-1}$ )
- $k_s$  thermal conductivity of solid ( $Wm^{-1}K^{-1}$ )
- $L$  length of the cavity ( $m$ )
- $Nu$  Nusselt number
- $n$  dimensional distances either  $x$  or  $y$  direction acting normal to the surface
- $N$  non-dimensional distances either  $X$  or  $Y$  direction acting normal to the surface
- $p$  dimensional pressure ( $Nm^{-2}$ )
- $P$  dimensionless pressure
- $Pr$  Prandtl number
- $Re$  Reynolds number
- $Ri$  Richardson number
- $Q$  non-dimensional heat-generating parameter
- $q$  uniform heat flux
- $T$  dimensional temperature ( $K$ )
- $\Delta T$  dimensional temperature difference ( $K$ )
- $u, v$  dimensional velocity components ( $ms^{-1}$ )
- $U, V$  dimensionless velocity components
- $\bar{V}$  cavity volume ( $m^3$ )
- $w$  height of the opening ( $m$ )
- $x, y$  Cartesian co-ordinates ( $m$ )
- $X, Y$  dimensionless Cartesian coordinates

### Greek symbols

- $\alpha$  thermal diffusivity ( $m^2s^{-1}$ )
- $\beta$  thermal expansion coefficient ( $K^{-1}$ )
- $\nu$  kinematic viscosity ( $m^2s^{-1}$ )
- $\theta$  non dimensional temperature
- $\rho$  density of the fluid ( $kgm^{-3}$ )

### Subscripts

- $av$  average
- $h$  heated wall
- $i$  inlet state